BRAIN
ORIGINAL ARTICLE

Hippocampal aggregation signatures of pathogenic *UBQLN2* in amyotrophic lateral sclerosis and frontotemporal dementia

Kyrah M. Thumbadoo,[1,2] Birger V. Dieriks,[2,3] Helen C. Murray,[2,3] Molly E. V. Swanson,[1,3] Ji Hun Yoo,[2,4] Nasim F. Mehrabi,[2,3] Clinton Turner,[2,3,5] Michael Dragunow,[2,4] Richard L. M. Faull,[2,3] Maurice A. Curtis,[2,3] Teepu Siddique,[6,7,8] Christopher E. Shaw,[2,9] Kathy L. Newell,[10] Lyndal Henden,[11] Kelly L. Williams,[11] Garth A. Nicholson[11,12,13,14] and Emma L. Scotter[1,2]

Pathogenic variants in the *UBQLN2* gene cause X-linked dominant amyotrophic lateral sclerosis and/or frontotemporal dementia characterized by ubiquilin 2 aggregates in neurons of the motor cortex, hippocampus and spinal cord. However, ubiquilin 2 neuropathology is also seen in sporadic and familial amyotrophic lateral sclerosis and/or frontotemporal dementia cases not caused by *UBQLN2* pathogenic variants, particularly *C9orf72*-linked cases. This makes the mechanistic role of mutant ubiquilin 2 protein and the value of ubiquilin 2 pathology for predicting genotype unclear. Here we examine a cohort of 44 genotypically diverse amyotrophic lateral sclerosis cases with or without frontotemporal dementia, including eight cases with *UBQLN2* variants [resulting in p.S222G, p.P497H, p.P506S, p.T487I (two cases) and p.P497L (three cases)].

Using multiplexed (five-label) fluorescent immunohistochemistry, we mapped the co-localization of ubiquilin 2 with phosphorylated TDP-43, dipeptide repeat aggregates and p62 in the hippocampus of controls ($n = 6$), or amyotrophic lateral sclerosis with or without frontotemporal dementia in sporadic ($n = 20$), unknown familial ($n = 3$), *SOD1*-linked ($n = 1$), *FUS*-linked ($n = 1$), *C9orf72*-linked ($n = 5$) and *UBQLN2*-linked ($n = 8$) cases.

We differentiate between (i) ubiquilin 2 aggregation together with phosphorylated TDP-43 or dipeptide repeat proteins; and (ii) ubiquilin 2 self-aggregation promoted by *UBQLN2* pathogenic variants that cause amyotrophic lateral sclerosis and/or frontotemporal dementia. Overall, we describe a hippocampal protein aggregation signature that fully distinguishes mutant from wild-type ubiquilin 2 in amyotrophic lateral sclerosis with or without frontotemporal dementia, whereby mutant ubiquilin 2 is more prone than wild-type to aggregate independently of driving factors. This neuropathological signature can be used to assess the pathogenicity of *UBQLN2* gene variants and to understand the mechanisms of *UBQLN2*-linked disease.

1 School of Biological Sciences, University of Auckland, Auckland 1010, New Zealand
2 Centre for Brain Research, University of Auckland, Auckland 1010, New Zealand
3 Department of Anatomy and Medical Imaging, University of Auckland, Auckland 1010, New Zealand
4 Department of Pharmacology and Clinical Pharmacology, University of Auckland, Auckland 1010, New Zealand
5 Department of Anatomical Pathology, LabPlus, Auckland City Hospital, Auckland 1010, New Zealand
6 Department of Neurology, Northwestern University Feinberg School of Medicine, Chicago, IL 60611, USA
7 Department of Cell and Developmental Biology, Northwestern University Feinberg School of Medicine, Chicago, IL 60611, USA
8 Department of Pathology, Northwestern University Feinberg School of Medicine, Chicago, IL 60611, USA

Received August 02, 2023. Revised March 03, 2024. Accepted March 07, 2024. Advance access publication May 4, 2024

9 UK Dementia Research Institute Centre, Institute of Psychiatry, Psychology and Neuroscience, King's College London, London SE5 8AF, UK
10 Department of Pathology and Laboratory Medicine, Indiana University School of Medicine, Indianapolis, IN 46202, USA
11 Macquarie University Motor Neuron Disease Research Centre, Macquarie Medical School, Faculty of Medicine, Health and Human Sciences, Macquarie University, Sydney, New South Wales 2109, Australia
12 Northcott Neuroscience Laboratory, Australian and New Zealand Army Corps (ANZAC) Research Institute, Concord, New South Wales 2139, Australia
13 Faculty of Medicine, University of Sydney, Sydney, New South Wales 2050, Australia
14 Molecular Medicine Laboratory, Concord Repatriation General Hospital, Concord, New South Wales 2139, Australia

Correspondence to: Emma L. Scotter
Building 110-427, 3A Symonds Street, School of Biological Sciences, University of Auckland, Auckland, New Zealand
E-mail: Emma.scotter@auckland.ac.nz

Keywords: *UBQLN2*; ubiquilin 2; amyotrophic lateral sclerosis (ALS); frontotemporal dementia (FTD); neuropathology; hippocampus

Introduction

UBQLN2 pathogenic variants are a rare cause of amyotrophic lateral sclerosis (ALS) with or without dementia, and the only known causal variants on the X-chromosome. *UBQLN2* (NM_013444) encodes the ubiquilin 2 protein, the best studied of five human ubiquilins, which contains a unique PXX domain comprising 12 proline-rich tandem repeats.[1,2] Like other ALS- and frontotemporal dementia (FTD)-linked degradation proteins [sequestosome 1/p62 (hereafter p62), valosin-containing protein, optineurin, and TANK-binding kinase 1], a key role for ubiquilin 2 is to bind ubiquitinated, misfolded and aggregated protein cargos, triaging them between the proteasome and autophagy intracellular degradation pathways.[3-6] New evidence suggests that ubiquilin 2 is intrinsically prone to self-assembly and undergoes reversible liquid-liquid phase separation, allowing it to bind ubiquitin-labelled proteins within phase-separated stress granules. It is postulated that upon ubiquitinated protein binding, ubiquilin 2 comes out of the liquid-droplet phase, bringing its cargo from the stress granule for delivery to the proteasome; ubiquilin 2 is therefore also implicated in stress granule disassembly.[7-10]

These roles at the interface between RNA processing and protein degradation—two key pathways in ALS and FTD pathogenesis—may underpin why ubiquilin 2 pathogenic variants cause disease. The majority of ALS and/or FTD (ALS/FTD)-causing *UBQLN2* missense variants are found within or flanking the PXX domain.[1,11-13] Altered residues within this region impair ubiquilin 2 binding to the proteasome and promote self-oligomerization and liquid-to-solid rather than liquid-liquid phase transition.[9,14-17] Numerous other variants have been identified in the ubiquitin-like domain, the stress-induced protein 1-like domains, or outside of known domains[18-37]; however, it is currently uncertain which of these *UBQLN2* variants are pathogenic.

The neuropathology of ALS/FTD caused by *UBQLN2* pathogenic variants is characterized by aggregated ubiquilin 2 in subregions of the neocortex, basal ganglia, medulla, spinal cord and hippocampal formation.[1,11,12,37-39] We previously found abundant ubiquilin 2-positive aggregates in the hippocampus of individuals with p.T487I *UBQLN2*-linked ALS+FTD, but not in cases of sporadic ALS.[38,39] However, ubiquilin 2 inclusions are not specific to *UBQLN2*-linked ALS/FTD cases and have been identified previously in sporadic and familial ALS, and ALS-dementia, regardless of whether ubiquilin 2 is wild-type or mutant.[1,11,12,37,38,40] Some of these ubiquilin 2 inclusions are immunopositive for other ALS/FTD-linked proteins, such as TAR DNA-binding protein-43 (TDP-43) or phosphorylated TDP-43 (pTDP-43), FUS, p62, optineurin or ubiquitin.[1,12,41-45] In addition, deposition of ubiquilin 2 in the hippocampus is a characteristic feature of ALS/FTD caused by *C9orf72* hexanucleotide repeat expansions, in which ubiquilin 2 is seen together with dipeptide repeat (DPR) proteins.[40] Thus, while ubiquilin 2 is clearly involved in ALS/FTD pathogenesis regardless of aetiology, the role of *UBQLN2* pathogenic variants and the predictive value of ubiquilin 2 labelling in relation to genotype is still unclear.

There is a clear need to determine whether *UBQLN2* pathogenic variants cause ubiquilin 2 neuropathology that is distinct from the wild-type ubiquilin 2 neuropathology seen in ALS/FTD with other genotypes. If they do, then defining a pathological signature for *UBQLN2*-linked disease will provide mechanistic insights and aid in assessment of the pathogenicity of *UBQLN2* genetic variants, which have not yet been confirmed to be causative. Because ubiquilin 2 aggregation across a range of ALS/FTD genotypes occurs in the hippocampus, this region may provide insight into the requirements for mutant and wild-type ubiquilin 2 aggregation. Here we map the hippocampal ubiquilin 2 protein deposition signature with respect to pTDP-43, the two most abundant *C9orf72*-linked DPR proteins, and p62, in ALS/FTD with and without *UBQLN2* pathogenic variants.

Materials and methods

Relatedness analysis

We first sought to collect genetic evidence for pathogenicity of the *UBQLN2* p.T487I variant in ALS/FTD. Genome-wide genotype data from the family of *UBQLN2*-linked ALS+FTD Case MN17 (Family FALS5) and another Australian family with an identical *UBQLN2* p.T487I variant (Family FALS14) were analysed to determine whether they inherited the variant from a common ancestor (pedigree in Supplementary Fig. 1, sample information in Supplementary Table 1). These two families were previously reported to share a haplotype identical-by-state over the *UBQLN2* locus,[12] but genealogy analysis had been unable to link the pedigrees. Three individuals from Family FALS5 [all affected, pedigree IDs Patients III:8, IV:9, IV:18 (MN17)] and two individuals from Family FALS14 [pedigree IDs Patient II:1 (unaffected) and Patient III:2 (affected)] underwent

single nucleotide polymorphism (SNP) genotyping using the Illumina Infinium Global Screening Array v2.0. Identity-by-descent (IBD) analysis was performed using XIBD software[46] with the combined HapMap Phase II and III European (CEU) cohort as a reference dataset. SNPs in high linkage disequilibrium ($r^2 > 0.95$) or SNPs with a low minor allele frequency (MAF < 0.01) were removed from analysis, as well as SNPs with missing genotype calls in two or more samples. SNPs ($n = 39\,002$) remained for analysis and 211 IBD segments >3 cM were identified. The degree of relationship was estimated for each pair of samples using the lengths of inferred IBD segments, as in Estimation of Recent Shared Ancestry[47] and categorized as previously described.[48]

Systematic review of *UBQLN2*-linked ALS/FTD neuropathology

Journal articles were identified using PubMed that were published between January 1993 and May 2023. Search terms were *UBQLN2*, ubiquilin 2, amyotrophic lateral sclerosis, and ALS, combined with neuropathology, tissue, or immunohistochemistry. Articles that did not contain ubiquilin 2 neuropathological information in post-mortem ALS/FTD human brain tissue, were not primary research articles, or were not published in English were excluded. Seven papers were identified from which neuropathological data for TDP-43, ubiquilin 2, ubiquitin, p62, *C9orf72*-linked DPR proteins, and FUS protein aggregates in the spinal cord and hippocampus were extracted and tabulated.

Patient demographics and hippocampal brain tissue

Formalin-fixed paraffin-embedded (FFPE) post-mortem hippocampal tissue from six neurologically normal and 30 ALS cases with or without FTD, processed as previously described,[49] were obtained from the Neurological Foundation Human Brain Bank at the Centre for Brain Research, Auckland, New Zealand (NZ). These included 20 cases with sporadic ALS (one with co-morbid FTD), three with familial ALS of unknown genotype, one with *SOD1*-linked ALS (p.E101G), five with *C9orf72*-linked ALS, and one with ALS+FTD with the *UBQLN2* p.T487I variant (pedigree ID Family FALS5 Patient IV:18 in Fig. 1A of Williams *et al.*[12] and in this report; coded MN17 in Fig. 1D of Scotter *et al.*[38] and in this report). Note that MN17 was stored in fixative for 7 years before embedding. All non-*SOD1*-linked NZ cases had confirmed pTDP-43 proteinopathy in the motor cortex. FFPE hippocampal tissue was also obtained from the Victoria Brain Bank, from a relative of the *UBQLN2* p.T487I case (p.T487I, ALS+FTD; pedigree ID V:7 in Fig. 1A of Williams *et al.*[12] and in this report); the London Neurodegenerative Diseases Brain Bank and Brains for Dementia from an unrelated *UBQLN2*-linked case (p.P506S, ALS+FTD; pedigree ID II.2 in Fig. 1B of Gkazi *et al.*[11]), a case with a *UBQLN2* variant of unknown significance (p.S222G, progressive supranuclear palsy; Supplemental_variant_data of Keogh *et al.*[50]) and a *FUS*-linked case (p.P525L, ALS) from the Northwestern University Feinberg School of Medicine, USA from another unrelated *UBQLN2*-linked case (p.P497H, ALS; pedigree ID V:I of Family 186 in Fig. 1A of Deng *et al.*[1]); and from the Indiana University School of Medicine, USA from three related *UBQLN2*-linked cases [p.P497L; pedigree IDs II:3 (ALS), III:3 (ALS+FTD) and IV:2 (ALS+FTD) of Family 1T in Fig. 1 of Fahed *et al.*[37]]. All clinical and neuropathological diagnoses were conducted as previously described.[1,11,12,38] Informed donor consent and ethical approvals were obtained at each site, as previously described.[1,11,12,38] All protocols were approved by the University of Auckland Human Participants Ethics Committee (New Zealand) and carried out as per approved guidelines. This study was also approved by the Human Research Ethics Committee of Macquarie University (520211013428875). Patient demographic and clinical information is described in the Supplementary material, 'Methods' section for *UBQLN2* variant cases and summarized for all cases in Supplementary Table 2.

Fluorescent immunohistochemistry and image acquisition

Multiplex fluorescent immunohistochemistry

Multiplex (five-label) immunohistochemistry was performed as previously described.[51-53] Briefly, tissue sections were cut with a microtome in the transverse plane at a thickness of 7–10 µm and mounted onto SuperFrost Plus slides (Thermo Fisher Scientific). Mounted sections were dried at room temperature for a minimum of 1 week before immunohistochemistry. Slides were heated to 60°C for 1 h on a hot plate, then dewaxed and rehydrated through a xylene-alcohol-water series: 100% xylene, 2 × 30 min; 100% ethanol, 2 × 15 min; 95%, 85%, 75% ethanol, 5 min each; water 3 × 5 min. Antigens were retrieved through immersion in 10 mM sodium citrate buffer (0.05% Tween 20, pH 6.0) in a pressure cooker (Retriever 2100, Electron Microscopy Sciences) at 120°C for 20 min and cooled to room temperature for 100 min. Sections were washed 3 × 5 min in 1 × PBS and wax borders were drawn with an ImmEdge Hydrophobic Barrier PAP pen. Sections were permeabilized in PBS-T (PBS with 0.2% Triton™ X-100) for 15 min at 4°C, followed by 3 × 5-min PBS washes. Lipofuscin autofluorescence was quenched using TrueBlack® Lipofuscin quencher (Biotium) 1:20 in 70% ethanol for at least 30 s followed by three vigorous water washes. Sections were blocked with 10% normal donkey serum (Thermo Fisher Scientific) in PBS for 1 h before 4°C overnight incubation with primary antibodies targeting ubiquilin 2, phosphorylated TDP-43 (pTDP-43), p62 and *C9orf72*-linked dipeptide repeat proteins polyGA and polyGP (Supplementary Table 3). Following PBS washes, species- and isotype-specific secondary antibodies and Hoechst 33342 nuclear stain (Supplementary Table 4) were applied for 3 h in 1% normal donkey serum at room temperature. After final 3 × 5-min PBS washes, sections were coverslipped with #1.5 coverslips (Menzel-Gläser) using ProLong™ Gold Antifade Mountant (Thermo Fisher Scientific). All primary antibodies used in this study have been previously validated in human brain tissue[6,38,54,55] and secondary antibodies showed no non-specific binding or signal bleed-through into adjacent channels (Supplementary Fig. 2) or cross-reactivity (Supplementary Fig. 3).

Multiplex (five-label) images were acquired using a Zeiss Z2 Axioimager with a MetaSystems VSlide slide scanning microscope (20× dry magnification lens, 0.9 NA) with a Colibri 7 solid-state fluorescent light source. Sections were imaged with the same exposure time and gain settings for each staining combination where possible. *UBQLN2*-linked ALS+FTD Case V:7-p.T487I showed consistently poor Hoechst immunoreactivity, while *UBQLN2*-linked ALS+FTD Case MN17-p.T487I showed poor immunoreactivity overall, likely due to long-term fixation, therefore a longer exposure was used for both cases when imaging. Single filters, as described and validated previously,[53] were used to excite fluorophores and detect the following wavelengths: filter Set 1 (LED 385; Em 447/60 nm), Set 3 (LED 475; Em 527/20 nm), Set 4 (LED 555; Em 580/23 nm), Set 5 (LED 590; Em 628/32 nm), Set 6 (LED 630; Em 676/29 nm) and Set 7 (LED 735; Em 809/81 nm) and visualized with MetaFer software (MetaSystems, v.3.12.1) equipped with a CoolCube 4 m TEC (monochrome) sCMOS digital camera. Image tiles were seamlessly

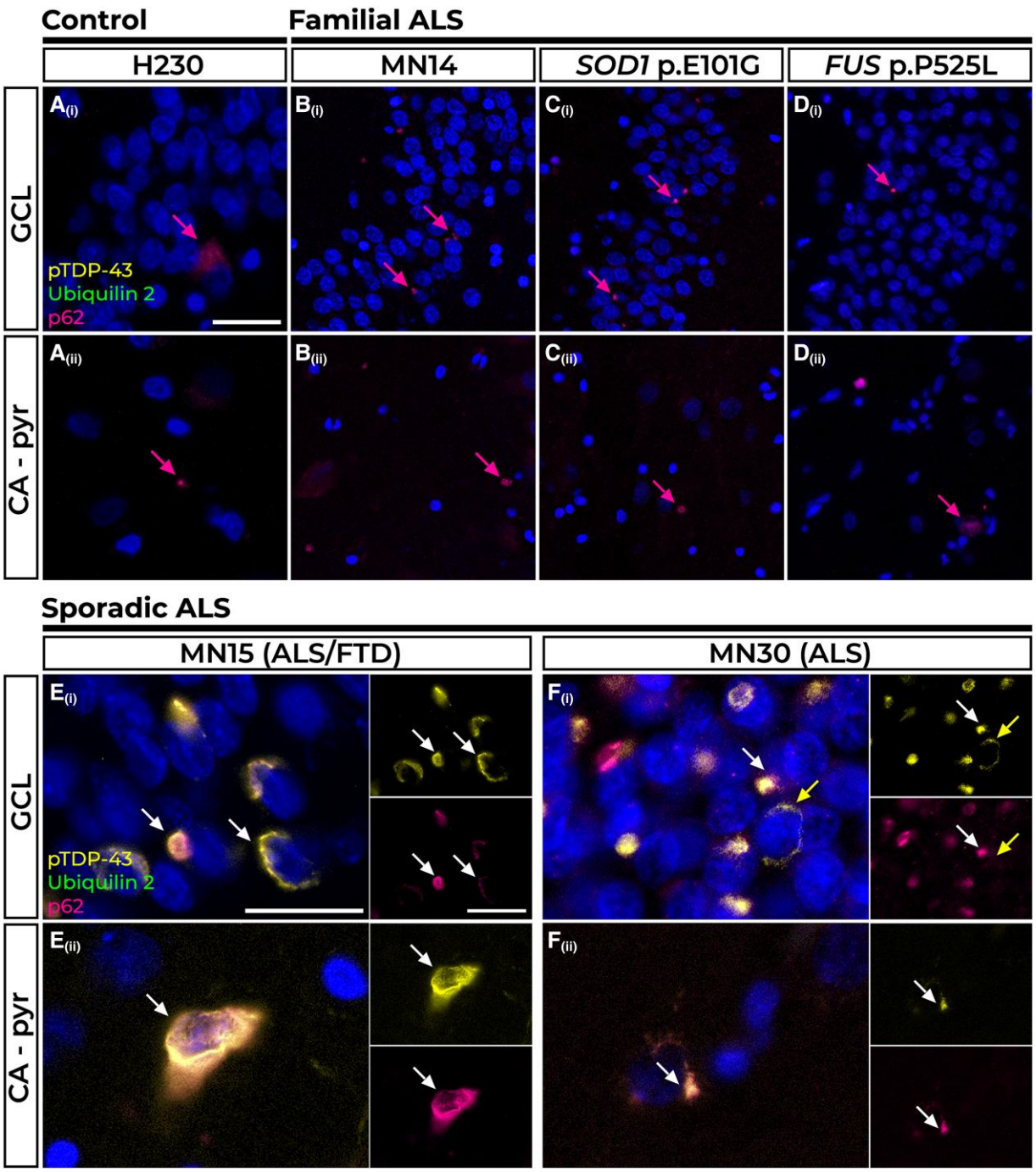

Figure 1 Pathology in the hippocampal dentate gyrus and cornu ammonis regions of control, familial and sporadic cases. The majority of control tissue had no pTDP-43 or ubiquilin 2 pathology, but one case had sparse p62 immunoreactivity in the granule cell layer (GCL) and cornu ammonis – pyramidal cells (CA – pyr) layers (**A** Control H230, pink arrows). Such p62-positive inclusions were also found in the GCL [**B(i)–D(i)**] and CA – pyr layers [**B(ii)–D(ii)**] in Case MN14, an amyotrophic lateral sclerosis (ALS) case of unknown genotypic cause (**B**), Case MN24, a *SOD1* p.E101G case (**C**) and Case P525L, a *FUS* p.P525L case (**D**). P62-positive perinuclear pTDP-43 aggregates negative for ubiquilin 2 were found in the GCL and CA – pyr regions of $n = 6$ sporadic cases represented here by ALS+FTD Case MN15 [**E(i** and **ii)**, white arrows] and ALS Case MN30 [**F(i** and **ii)**, white arrows]. Rare pTDP-43 aggregates negative for p62 are indicated by the yellow arrow in **F(ii)**. Scale bars = 50 µm (**A–D**); and 25 µm (**E** and **F**). FTD = frontotemporal dementia.

stitched using MetaCyte software and stitched images were extracted using VSViewer software (MetaSystems, v.1.1.106).

Double-label immunohistochemistry

For super-resolution stimulated emission depleted (STED) microscopy of *C9orf72*-linked ALS Case MN28, double-label immunohistochemistry was performed. Immunohistochemistry was performed as described above with primary antibody targeting ubiquilin 2 and detected by goat anti-mouse IgG_{2a} Alexa Fluor 594, but with primary antibody targeting polyGA detected by goat anti-mouse IgG_1 Biotin (A10519, Thermo Fisher Scientific), followed by 3×5-min PBS washes and an additional incubation with Star Red neutravidin (STRED-0121, Abberior) for 1 h at room temperature.

After final 3 × 5-min PBS washes, sections were coverslipped with #1.5 coverslips using ProLong™ Glass Antifade Mountant (P36984, Thermo Fisher Scientific).

STED images were acquired using an Abberior Facility STED microscope (60× UPLXAPO oil immersion lens, 1.42 NA) using ImSpector Lightbox software (Specim, v.16.3.13779). A 561-nm pulsed diode laser was used to excite Alexa Fluor 594 and a 640-nm diode laser was used to excite Star Red Neutravidin. For STED imaging, a pulsed 775-nm laser was used for depletion of both fluorophores. After scanning, the images were processed using the PureDenoise plugin[56] for ImageJ (National Institutes of Health, USA v1.53f51).

Final figures of multiplex and double-label immunohistochemistry were compiled using Adobe Photoshop CC (Adobe Systems Incorporated, v24.4.1). For clarity, multiplex labels are shown in separate panels, either pTDP-43, ubiquilin 2 and p62, or ubiquilin 2, polyGA and polyGP, with negative labelling not shown.

Results

UBQLN2 p.T487I variant in ALS/FTD Families FALS5 and FALS14 is pathogenic and was inherited from a common ancestor

Since the initial report by Williams *et al.*[12] of an identical *UBQLN2* p.T487I variant in ALS Families FALS5 and FALS14, we report here that Cases MN17 (IV:18) and V:7 from Family FALS5 developed ALS+FTD, indicating that FTD is part of the clinical phenotype in that family. To examine relatedness between the families and confirm that *UBQLN2* p.T487I arose in a common founder, we performed IBD analysis. IBD segments were identified over the *UBQLN2* locus between all four affected individuals from both families (Table 1), while there were no IBD segments inferred over *UBQLN2* between the affected individuals from Family FALS5 and the unaffected individual from Family FALS14, who did not carry *UBQLN2* p.T487I. The interval shared by all four affected individuals spanned rs952836 to rs6423133 and was 68 cM in length. This confirms a founder effect of *UBQLN2* p.T487I in Families FALS5 and FALS14. The genotyped individuals across these families are estimated to be fourth to fifth degree relatives (first cousins once removed – second cousins) (Table 2), now confirming segregation of the *UBQLN2* p.T487I variant in 18 individuals from the proposed combined Australia-New Zealand pedigree and providing irrefutable genetic evidence that *UBQLN2* p.T487I is pathogenic for ALS/FTD.

Ubiquilin 2 labelling in previous studies failed to discriminate between *UBQLN2*-linked and other genotypes of ALS/FTD

Systematic review of the literature describing ubiquilin 2 neuropathology in human ALS/FTD identified 137 results, of which seven articles met the criteria for full review. The hippocampal neuropathology of ubiquilin 2 with respect to five other ALS/FTD-linked proteins is summarized in Table 3. Ubiquilin 2 aggregate deposition in the hippocampal molecular layer was most frequently reported upon, being found in *UBQLN2*-linked and *C9orf72*-linked ALS/FTD, sometimes together with ubiquitin or p62.[6] Ubiquilin 2 aggregate

Table 1 IBD segments inferred over UBQLN2 on the X chromosome (chromosome 23)

Individual 1		Individual 2		StartSNP	EndSNP	Start Pos(bp)	End Pos(bp)
Family ID	Pedigree ID	Family ID	Individual ID				
FALS5	III:8	FALS5	IV:9	rs17330993	rs11156600	2779749	154440161
FALS5	III:8	FALS5	IV:18[a]	rs7062445	rs6423133	19650411	123608292
FALS5	III:8	FALS14	III:2	rs952836	rs17315029	40344087	129605268
FALS5	IV:9	FALS5	IV:18	rs6628597	rs6423133	31382037	123608292
FALS5	IV:9	FALS14	III:2	rs952836	rs17277770	40344087	132774456
FALS5	IV:18	FALS14	III:2	rs952836	rs6423133	40344087	123608292

IBD = identical by descent; SNP = single nucleotide polymorphism.
[a]FALS5 IV:18 is referred to as Case MN17 in this report.

Table 2 Estimated degree of relatedness and fraction of genome with zero, one and two alleles identical-by-descent (IBD) between all samples in UBQLN2 p.T487I-linked Families FALS5 and FALS14

–	Individual 1		Individual 2		Fraction IBD = 0	Fraction IBD = 1	Fraction IBD = 2	Degree[a]
	Family ID	Pedigree ID	Family ID	Individual ID				
Intra-family	FALS5	III:8	FALS5	IV:9	0.529	0.471	0	2
	FALS5	III:8	FALS5	IV:18[b]	0.529	0.471	0	2
	FALS5	IV:9	FALS5	IV:18	0.751	0.249	0	3
	FALS14	II:1	FALS14	III:2	0.515	0.485	0	2
Inter-family	FALS5	III:8	FALS14	II:1	0.877	0.123	0	4
	FALS5	III:8	FALS14	III:2	0.927	0.073	0	5
	FALS5	IV:9	FALS14	II:1	0.942	0.058	0	5
	FALS5	IV:9	FALS14	III:2	0.948	0.052	0	5
	FALS5	IV:18	FALS14	II:1	0.926	0.074	0	5
	FALS5	IV:18	FALS14	III:2	0.948	0.052	0	5

[a]Degrees of relatedness as per Ramstetter *et al.*[48]: 2 = grandparent-grandchild, avuncular, half-sibling; 3 = first cousin, great-grandparent, grand-avuncular; 4 = first cousin once removed, great grandparent-grandparent; 5 = second cousin, first cousin twice removed.
[b]FALS5 IV:18 is referred to as Case MN17 in this report.

Table 3 Hippocampal ubiquilin 2 labelling in previous studies failed to discriminate between UBQLN2-linked and other genotypes of ALS/FTD

Region of hippocampal formation	ML						GCL						CA					
Reported protein pathology	Ubiquilin 2	TDP-43	Ubiquitin	p62	DPRs	FUS	Ubiquilin 2	TDP-43	Ubiquitin	p62	DPRs	FUS	Ubiquilin 2	TDP-43	Ubiquitin	p62	DPRs	FUS
***UBQLN2*-linked ALS/FTD**																		
Deng *et al.*[1] p.P506T	+		+				−						+		+			
Gkazi *et al.*[11] p.P506S							+	+										
Wu *et al.*[6] p.P506S	+			+														
Wu *et al.*[6] p.P497H	+			+														
Fahed *et al.*[37] p.P497L	+						−											
Scotter *et al.*[38] p.T487I	+	−			−		−	−			−							
Wu *et al.*[6] p.T487I	+			+														
Williams *et al.*[12] p.T487I																		
Non *UBQLN2*-linked ALS/FTD																		
Deng *et al.*[1] ALS-dementia[a]	+	−	+			−	+	+	+	+		−	+	−	+	+		
Brettschneider *et al.*[40] *C9orf72*	+	−		+	−		+	+			+		+				+	
Brettschneider *et al.*[40] Non-*C9orf72*							+	+										
Scotter *et al.*[38] *C9orf72*	+	−					+	−			+		+				+	
Scotter *et al.*[38] sALS	−	−			−		−	−			−							
Gkazi *et al.*[11] sALS							+											

ALS = amyotrophic lateral sclerosis; CA = cornu ammonis; DPRs = dipeptide repeat proteins; FTD = frontotemporal dementia; GCL = granule cell layer; ML = molecular layer; sALS = sporadic ALS; +/− = presence/absence of pathology.
[a]*C9orf72*-linked.

deposition in the granule cell layer (GCL) of the hippocampal dentate gyrus was inconsistent between cases of *UBQLN2*-linked ALS/FTD but was found in all cases of 'ALS-dementia' in Deng *et al.*[1] (all later confirmed to be *C9orf72*-positive) and in a single sporadic ALS/FTD case.[11] Cornu ammonis (CA) ubiquilin 2 pathology had been reported in both *UBQLN2*-linked and *C9orf72*-linked ALS/FTD.[1,38,40] Overall, neither ubiquilin 2 staining alone, nor in combinations previously tested, could distinguish mutant ubiquilin 2 aggregation in *UBQLN2*-linked ALS/FTD from wild-type ubiquilin 2 aggregation in other ALS/FTD genotypes.

Ubiquilin 2 and other pathology in ALS/FTD of various genotypes

P62 pathology in control and familial ALS cases

Five of the six non-neurodegenerative disease control cases included in this study showed no deposition of ubiquilin 2, pTDP-43, p62 or DPR protein aggregates in any region of the hippocampus (not shown). The remaining control case (Case H230) showed sparse p62 aggregates in the GCL and CA pyramidal cell layer (CA – pyr) [Fig. 1A(i and ii)].

All five non-*UBQLN2* non-*C9orf72* familial ALS cases also showed sparse p62 aggregates in the GCL and CA – pyr regions; three cases were of unknown genotype, represented by Case MN14 [Fig. 1B(i and ii)], one harboured a *SOD1* p.E101G pathogenic variant [Fig. 1C(i and ii)] and one harboured a *FUS* p.P525L pathogenic variant [Fig. 1D(i and ii)]. No other pathology was observed in familial cases in hippocampal regions (note that neither anti-FUS nor anti-SOD1 antibodies were used).

pTDP-43 and p62 pathology in sporadic ALS cases

None of the 20 sporadic ALS cases (one with co-morbid FTD) showed hippocampal ubiquilin 2 or DPR aggregates (not shown). Fourteen cases (70%) were devoid of either ubiquilin 2 or pTDP-43 in the GCL, molecular layer (ML), CA – pyr and cornu ammonis – lacunosum-molecular and radiatum (CA – l-m/rad, hereafter 'CA – dendritic layers') (not shown); however, four of these cases (20%) had compact p62-positive neuronal cytoplasmic inclusions (NCIs) in the GCL and CA – pyr regions that were negative for all other markers (Supplementary Fig. 4). Six cases (30%; including representative Cases MN15 with ALS+FTD and MN30 with ALS) had compact or net-like perinuclear pTDP-43-positive NCIs in the GCL and CA – pyr regions ranging in density from sparse to frequent, suggestive of stage 4 pTDP-43 proteinopathy.[57] These pTDP-43 aggregates were almost always p62 positive and ubiquilin 2 negative [Fig. 1E(i and ii) and F(i and ii), white arrows, with the exception of 1–2 perinuclear aggregates that were not p62 labelled [Fig. 1F(i), yellow arrow].

Ubiquilin 2, p62, DPR protein and rare pTDP-43 pathology in C9orf72 cases

Four of the five *C9orf72*-linked ALS cases showed identical hippocampal pathology (represented by Case MN18), while the fifth case (Case MN28) differed by additionally having pTDP-43 aggregates in the GCL and CA – apyr, described below.

All five cases shared a signature of numerous ubiquilin 2 aggregates in the ML, GCL and CA – dendritic regions. In general, the molecular layers (ML and CA – dendritic layers) showed similar pathological patterns to one another, while of the cellular layers (GCL and CA – pyr cell soma layers) the GCL showed variable pTDP-43 and denser DPR-p62 pathology that incorporated ubiquilin 2. In the ML and CA – dendritic layers, ubiquilin 2 aggregates were punctate or wispy, dendritic and very rarely co-localized with p62 [Fig. 2A(i and ii) and B(i and ii), green arrowheads] and never with DPR proteins [Fig. 2C(i and ii) and D(i and ii), green arrowheads]. In the CA – pyr, aggregates did not contain ubiquilin 2 [Fig. 2A(iii)–D(iii)] but were positive for p62 [Fig. 2A(iii) and B(iii), pink arrows], poly(glycine-arginine) (polyGA) and poly(glycine-proline) (polyGP) [Fig. 2C(iii) and D(iii), orange arrows and insets], with pTDP-43 also seen in Case MN28, albeit rarely [Fig. 2B(iii), yellow arrow].

In the GCL, ubiquilin 2 aggregates were perinuclear NCIs that were negative for pTDP-43 (except rare aggregates in Case MN28, as below), but always positive for p62 [Fig. 2A(iv) and B(iv), white arrows and yellow arrow] and for polyGA but rarely polyGP [Fig. 2C(iv) and D(iv), purple arrows]. By two-colour super-resolution microscopy, ubiquilin 2 in the GCL of Case MN28 was either enmeshed with polyGA (Fig. 2E) or encircled it (Fig. 2F). Ubiquilin 2 aggregates positive for pTDP-43 were rare (1–2 GCL cells per section of Case MN28) and comprised a pTDP-43 'shell' surrounding polyGA either with polyGP (Supplementary Fig. 5A, white arrow) or without polyGP (Supplementary Fig. 5A, purple arrow). This supports a previous report that ubiquilin 2 in *C9orf72*-linked cases rarely co-localises with GCL pTDP-43, doing so only when DPR proteins are present in the aggregate.[58] Therefore, wild-type ubiquilin 2 aggregation may be 'seeded' in the GCL by polyGA rather than by pTDP-43.

Ubiquilin 2, p62 and pTDP-43 pathology in UBQLN2 cases

All seven *UBQLN2*-linked ALS/FTD cases showed signature ubiquilin 2-positive but pTDP-43-negative punctate aggregates in the hippocampal ML and CA – dendritic layers, albeit at variable loads [Fig. 3A(i and ii), B(i and ii), C(i and ii), D(i and ii), E(i and ii), F(i and ii) and G(i and ii), white arrows]. Similar to *C9orf72* cases, the molecular layers (ML and CA – dendritic layers) of *UBQLN2* cases showed comparable neuropathology to one another. In the ML, ubiquilin 2 aggregates were punctate and appeared to be localized to the dendritic spines of the granule cells, as reported in *UBQLN2*-linked ALS/FTD and mutant *UBQLN2* rodent models.[1,59] In contrast to *C9orf72*-linked cases, these ML ubiquilin 2 aggregates almost always co-localized with p62, as did punctate ubiquilin 2 aggregates in the CA – dendritic layers [Fig. 3A(i and ii), B(i and ii), C(i and ii), D(i and ii), E(i and ii), F(i and ii) and G(i and ii), inset images]. The PSP case with a *UBQLN2* p.S222G variant of unknown significance did not share this signature of ubiquilin 2– and p62-positive aggregates in the ML and CA – dendritic layers, instead having p62-only aggregates in the CA – dendritic layers [Fig. 3H(i and ii), pink arrowheads].

Confocal microscopy of the ML and CA – dendritic layers confirmed that the p62-positive mutant ubiquilin 2 aggregates in *UBQLN2*-linked ALS/FTD cases (Supplementary Fig. 6A, representative p.P506S case shown) differed from wild-type ubiquilin 2 aggregates in those regions in *C9orf72*-linked ALS, which were predominantly p62 negative (Supplementary Fig. 6B, representative Case MN28). Further, while mutant ubiquilin 2 in *UBQLN2*-linked cases formed small compact aggregates (Supplementary Fig. 6A) wild-type ubiquilin 2 in *C9orf72*-linked cases formed small compact aggregates and wispy skein-like structures (Supplementary Fig. 6B). Therefore, mutant but not wild-type ubiquilin 2 in the hippocampal ML and CA – dendritic layers may promote or scaffold the co-aggregation of p62 and there may be structural differences between mutant and wild-type.

In the cellular layers, the GCL generally showed similar but denser pathology than that of the CA – pyr region for a given case, but neuropathology in these layers was highly variable between cases. Cases P497H, MN17 – T487I and V:7 – T487I had no pathology in the

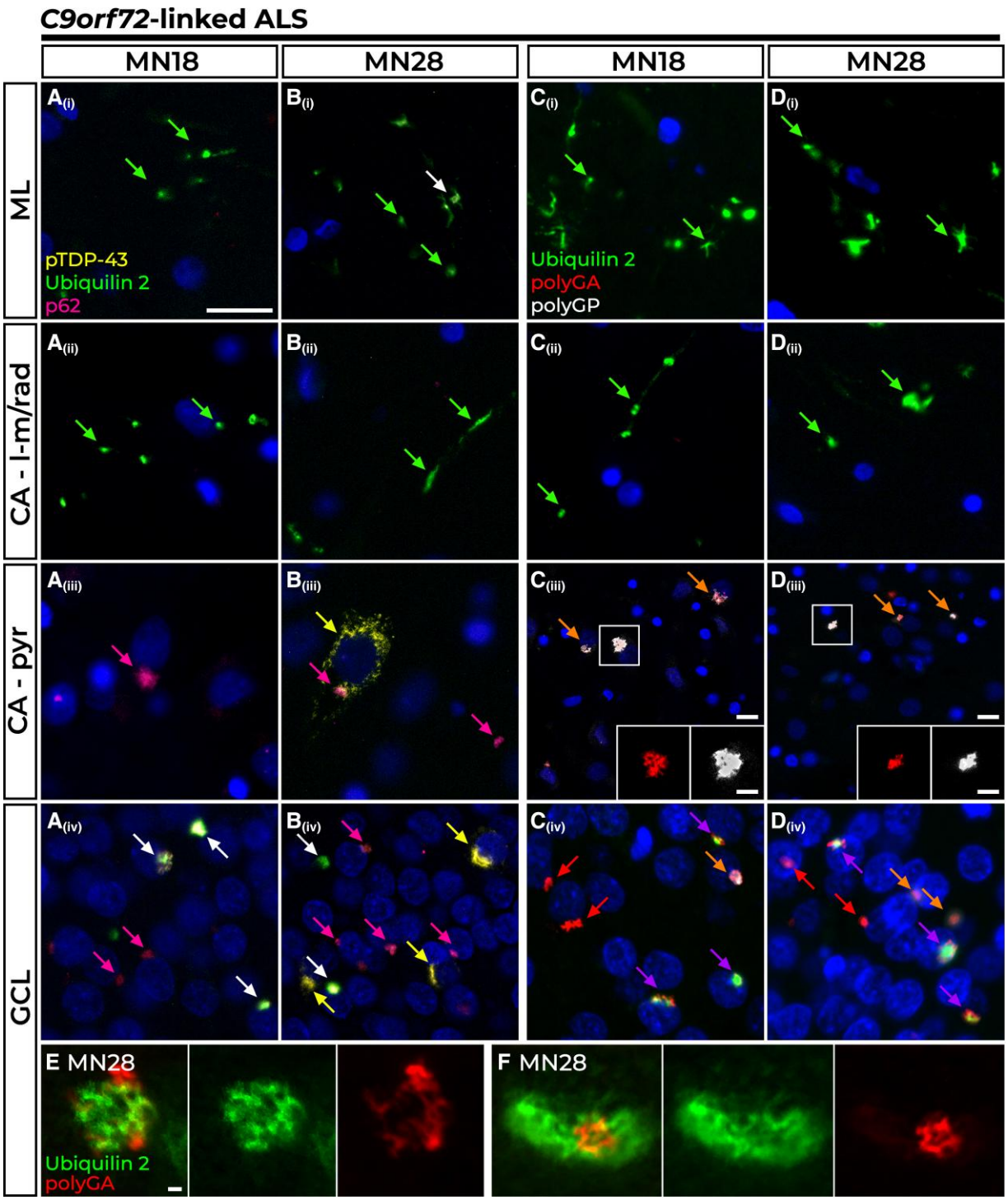

Figure 2 Pathology in the hippocampal dentate gyrus and cornu ammonis regions of *C9orf72*-linked cases. All *C9orf72*-linked amyotrophic lateral sclerosis/frontotemporal dementia (ALS/FTD) cases showed wispy ubiquilin 2 aggregates in the molecular layer (ML) and cornu ammonis – lacunosum-molecular and radiatum (CA – l-m/rad) layers that were predominantly p62 negative [**A(i** and **ii)** and **B(i** and **ii)**, green arrows], with larger aggregates sometimes co-labelling with p62 in the ML [**B(i)**, white arrow]. In Case MN18, representative of $n = 4$ *C9orf72* cases (80%), the CA – pyr (pyramidal) cells harboured stellate p62 aggregates [**A(iii)**, pink arrow] while the GCL showed stellate p62 aggregates either with ubiquilin 2 [**A(iv)**, white arrows] or without [**A(iv)**, pink arrow]. Case MN28 shared this pattern of p62 and ubiquilin 2 pathology with the additional presence of perinuclear pTDP-43 inclusions, often found without other co-labelling in the CA – pyr region [**B(iii)**, yellow arrow] or granule cell layer (GCL) [**B(iv)**, yellow arrow]. Ubiquilin 2 aggregates in the ML and CA –l-m/rad layers were negative for dipeptide repeat proteins in all *C9orf72* cases [**C(i** and **ii)** and **D(i** and **ii)**, green arrows]. The dominant pathology in CA – pyr regions was the presence of polyGA and polyGP inclusions negative for ubiquilin 2 [**C(iii)** and **D(iii)**, orange arrowheads]. All GCL ubiquilin 2 was co-localized with at least one dipeptide repeat protein [**C(iv)** and **D(iv)**, purple arrows]. Ubiquilin 2-negative aggregates were comprised of both dipeptide repeat proteins [**C(iv)** and **D(iv)**, orange arrows] or most commonly, polyGA without other co-labelling [**C(iv)** and **D(iv)**, red arrows]. Super-resolution STED microscopy of ubiquilin 2-positive polyGA aggregates in the GCL of Case MN28 demonstrated polyGA enmeshed with and encircling ubiquilin 2 (**E**) or ubiquilin 2 labelling around a core of polyGA (**F**). Scale bar in main images **A–D** = 50 µm; magnifications in **C(iv)** and **D(iv)**, 25 µm; and 1 µm in **E** and **F**.

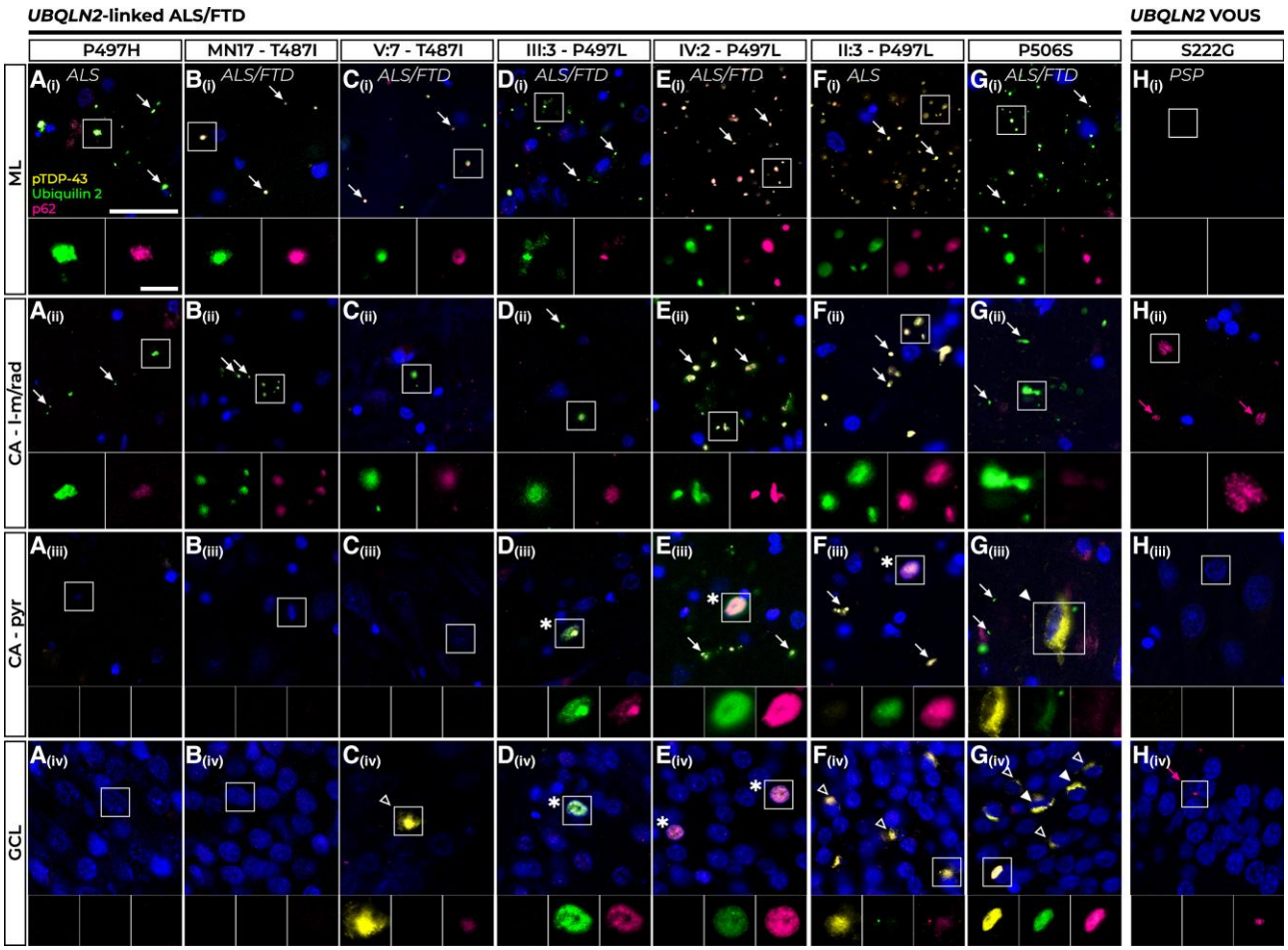

Figure 3 Pathology in the hippocampal dentate gyrus and cornu ammonis regions of *UBQLN2*-linked cases. All *UBQLN2*-linked amyotrophic lateral sclerosis/frontotemporal dementia (ALS/FTD) cases showed numerous p62-positive ubiquilin 2 aggregates, indicated by white arrows, in the molecular layer (ML) [**A(i)**–**G(i)**] and cornu ammonis – lacunosum-molecular and radiatum (CA – l-m/rad) layers [**A(ii)**–**G(ii)**]. Cases P497H and MN17-T487I showed no aggregate labelling in the CA – pyr (pyramidal) cells [**A(iii)** and **B(iii)**] or granule cell layer (GCL) [**A(iv)** and **B(iv)**]. ALS+FTD Case V:7 – T487I showed no pathology in the CA – pyr cells [**C(iii)**] and very rare p62-positive pTDP-43 aggregates negative for ubiquilin 2 in the GCL [**C(iv)**, hollow white arrowhead]. All three p.P497L mutant cases had rare intranuclear p62-positive ubiquilin 2 inclusions negative for pTDP-43 in the CA – pyr cells [**D(iii)**–**F(iii)**] and Cases III:3 – P497L and IV:2 – P497L also showed these in the GCL [**D(iv)** and **E(iv)**, all indicated by asterisk]. In Case II:3 – P497L no such intranuclear inclusions were observed in the GCL but frequent p62-positive pTDP-43 aggregates were seen instead [**F(iv)**, hollow arrowheads]. Case P506S had aggregates positive for p62, pTDP-43 and ubiquilin 2 in the CA – pyr cells [**G(iii)**, filled white arrowhead] and the GCL [**G(iv)**, filled white arrowheads] and numerous compact p62-positive but ubiquilin 2-negative pTDP-43 aggregates in the GCL [**G(iv)**, hollow white arrowheads]. A progressive supranuclear palsy (PSP) case harbouring a *UBQLN2* p.S222G variant of uncertain significance (VOUS) (**H**) had no pathology in the ML [**H(i)**] or CA – pyr cells [**H(iii)**], but showed sparse p62 positivity (pink arrows) in the CA – l-m/rad layers [**H(ii)**] and granule cell layer (GCL) [**H(iv)**]. Scale bar in main images = 25 µm; magnifications, 5 µm.

CA – pyr cells [Fig. 3A(iii), B(iii) and C(iii)], with Cases P497H and MN17 – T487I also having no pathology in the GCL [Fig. 3A(iv) and B(iv)], consistent with previous findings.[1,38] In contrast, Case V:7 – T487I showed very sparse pTDP-43 cytoplasmic aggregates in the GCL that were negative for ubiquilin 2 but weakly positive for p62 [Fig. 3C(iv), white hollow arrowhead]. All three cases harbouring a p.P497L variant showed rare p62-positive ubiquilin 2 intranuclear inclusions negative for pTDP-43 in the CA – pyr cells [Fig. 3D(iii), E(iii) and F(iii)]. Cases III:3 – P497L and IV:2 – P497L had these same intranuclear inclusions in the GCL at varying loads [Fig. 3D(iv) and E(iv)]. Consistent with the known spectrum of pTDP-43 loads in the GCL in ALS/FTD,[57] Case II:3 – P497L had no p62-positive ubiquilin 2 intranuclear inclusions but instead harboured abundant p62-positive cytoplasmic pTDP-43 aggregates, mostly negative for ubiquilin 2 [Fig. 3F(iv), white hollow arrowheads]. *UBQLN2*-linked ALS/FTD Case P506S had sparse pTDP-43 aggregates in the CA – pyr cells which were positive for ubiquilin 2 and faintly positive for p62 [Fig. 4G(iii), white filled arrowhead], while in the GCL it had abundant p62-positive pTDP-43 cytoplasmic aggregates that either co-localized with ubiquilin 2 [Fig. 3G(iv), white filled arrowheads] or were independent of ubiquilin 2 [Fig. 3G(iv), white hollow arrowheads]. Mutant ubiquilin 2 cytoplasmic aggregation in the GCL could therefore likely be scaffolded or 'seeded' by pTDP-43 when present. The *UBQLN2* p.S222G PSP case showed no pathology in the CA – pyr cells and sparse p62-only aggregates in the GCL that were not seen in *UBQLN2*-linked ALS/FTD cases [Fig. 3H(iii and iv), pink arrows].

All *UBQLN2* variant cases were negative for DPRs (not shown).

Combined pathological signatures discriminate between sporadic, *C9orf72*-linked and *UBQLN2*-linked ALS/FTD

Integration of all neuropathological findings (Supplementary Fig. 7) revealed a characteristic hippocampal neuropathological signature

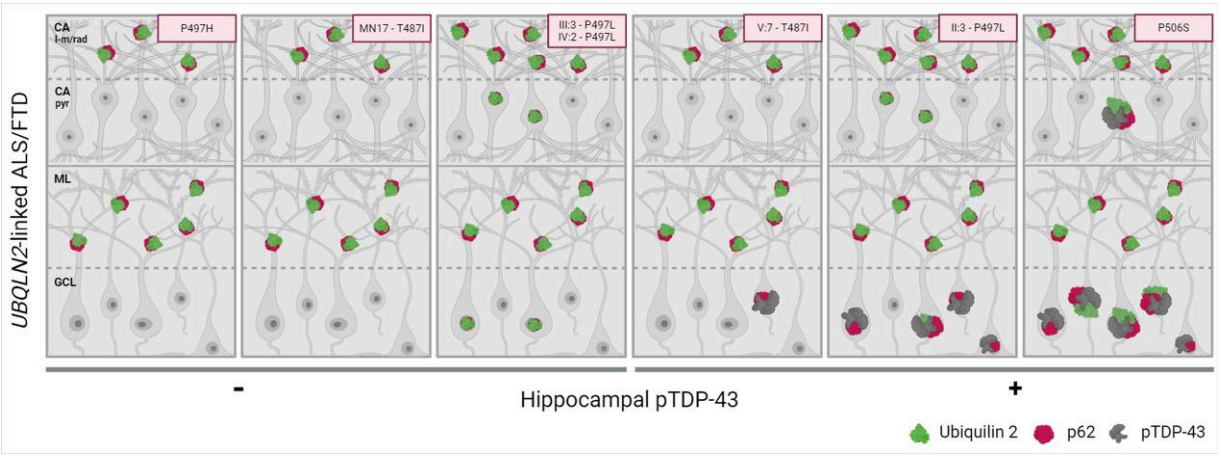

Figure 4 Schematic representation of the hippocampal neuropathological signature defining *UBQLN2*-linked ALS/FTD. In all *UBQLN2*-linked amyotrophic lateral sclerosis/frontotemporal dementia (ALS/FTD) cases, mutant ubiquilin 2 forms punctate, p62-positive aggregates in the cornu ammonis – lacunosum-molecular and radiatum (CA – l-m/rad) layers and molecular layer (ML), comprising a unique neuropathological signature. The neuropathology in the CA – pyr layer and granule cell layer (GCL) is variable between cases. The CA – pyr may show intranuclear p62-positive ubiquilin 2 aggregates (all three P497L cases) or aggregates positive for p62, pTDP-43 and ubiquilin 2 (Case P506S). The GCL may show intranuclear p62-positive ubiquilin 2 aggregates (Cases III:3 and IV:2 – P497L) or pTDP-43 aggregates that are frequent and ubiquilin 2-labelled (Cases p.P506S and II:3 – P497L) and/or rare and ubiquilin 2-negative (Cases p.P506S, II:3 – P497L, and V7 – p.T487I), suggesting a pathological cascade in which granule cell layer pTDP-43 aggregates provide a scaffold around which mutant ubiquilin 2 can aggregate. Image created in Biorender.com.

for *UBQLN2*-linked ALS/FTD that was distinct from that in other forms of ALS/FTD. Sporadic ALS cases were wholly devoid of hippocampal ubiquilin 2 or DPR protein pathology, with a minority of cases ($n = 6$) showing pTDP-43 aggregates in the granule cells that were ubiquilin 2 negative. Thus, wild-type ubiquilin 2 is not seeded/scaffolded to aggregate by cytoplasmic pTDP-43 aggregation. *C9orf72*-linked cases showed ML and CA – dendritic layer ubiquilin 2 aggregates that were wispy or punctate and predominantly p62 negative, while *UBQLN2*-linked cases showed ML and CA – dendritic layer ubiquilin 2 aggregates that were punctate and predominantly p62 positive. Mutant ubiquilin 2 aggregates thus promote the co-aggregation of p62 and this may relate to their conformational differences. Overall, mutant ubiquilin 2 causes unique neuropathology that is shared by cases harbouring p.T487I, p.P497H, p.P497L or p.P506S variants (Fig. 4). The absence of this signature in a case harbouring a p.S222G variant manifesting with PSP suggests this neuropathology can be used to discriminate pathological ALS/FTD-causing *UBQLN2* variants.

Ubiquilin 2 hippocampal pathology was present in both *UBQLN2*-linked ALS/FTD and *C9orf72*-linked ALS, but these genotypes could be discriminated when ubiquilin 2 was co-labelled with pTDP-43, DPR proteins, or p62. *C9orf72*-linked cases showed no ubiquilin 2 pathology in the CA – pyr cells, but always showed GCL ubiquilin 2 that co-localized with DPR aggregates but rarely pTDP-43. This supports the lack of seeding of wild-type ubiquilin 2 aggregation by pTDP-43 but suggests that wild-type ubiquilin 2 can be seeded by polyGA. In contrast, certain *UBQLN2*-linked cases showed that GCL ubiquilin 2 could co-localize with pTDP-43 when present. Therefore, mutant ubiquilin 2 is more aggregation-prone than wild-type, being seeded by pTDP-43.

Discussion

ALS shows considerable clinical, pathological and genetic heterogeneity.[60-62] While TDP-43 proteinopathy is seen in 97% of cases,[41,44,63] ALS/FTD-causing genetic variation can cause deposition of the encoded mutant protein leading to additional pathological aggregate signatures. We previously exploited this to infer *C9orf72* repeat expansion genotypes[64,65] through neuropathological screening of our New Zealand ALS cases.[38] Mutant *SOD1*,[66,67] *FUS*[45] and certain other genotypes[68,69] can also be inferred from neuropathology. However, no completely discriminating neuropathology has been reported for many ALS/FTD genes—particularly those such as *TARDBP*, *SQSTM1* and *UBQLN2* that encode proteins already within the hallmark TDP-43 inclusions.[43,68,70-74] This has hampered the validation of pathogenicity of novel variants in these genes, in turn obscuring understanding of protein domains and molecular processes important to ALS/FTD pathogenesis. However, we report here a unique neuropathological signature for mutant ubiquilin 2 in the hippocampus that discriminates *UBQLN2*-linked ALS/FTD cases from all others tested.

pTDP-43 in *UBQLN2*-linked cases: an independent pathology

Before discussing the unique pattern of hippocampal ubiquilin 2 pathology shared by *UBQLN2*-linked cases, it must first be noted that pTDP-43 deposition was variable. Four of the seven *UBQLN2*-linked ALS/FTD cases were devoid of GCL pTDP-43 aggregates (Cases P497H, MN17-T487I, III:3 – P497L and IV:2 – P497L), one case had very sparse GCL pTDP-43 aggregates that were ubiquilin 2 negative (Case V:7-T487I) and two cases showed frequent GCL pTDP-43 aggregates that were mostly ubiquilin 2 negative (Case II:3 – P497L) or that were mostly ubiquilin 2 positive (Case P506S). Although pTDP-43 aggregates are nearly ubiquitous in the ALS spinal cord and motor cortex, only in ~15%–30% of ALS cases are they found in the hippocampus.[57,75] Our findings suggest that variable regional pTDP-43 deposition occurs in the context of *UBQLN2*-linked ALS/FTD, just as it does in sporadic and *C9orf72*-linked ALS/FTD.

Wild-type ubiquilin 2 pathology in *C9orf72*-linked cases

Hippocampal ubiquilin 2 deposition is a known and striking feature of *C9orf72*-linked ALS/FTD.[40] In our *C9orf72*-linked ALS cases, large

stellate GCL ubiquilin 2 was found to preferentially co-localize with the aggregation-prone polyGA DPR protein compared to polyGP. Furthermore, polyGP aggregates were very rarely independent of polyGA. These findings support the emerging consensus that polyGA aggregates 'seed' polyGP protein aggregation.[76-78] Similar observations were made by Mackenzie and colleagues[58] of aggregates with a core of polyGA surrounded by an aggregated TDP-43 shell; a finding recapitulated here and supported by *in vitro* work showing polyGA aggregation preceding TDP-43 accumulation.[79] The ability of DPR proteins to seed ubiquilin 2 however, appears more complex. We previously showed ubiquilin 2 at the core of polyGP-positive aggregates, but we did not co-label for polyGA.[38] STED imaging in the current study shows that ubiquilin 2 may either surround polyGA or be enmeshed with it, suggesting that in *C9orf72*-linked ALS pathogenesis, the interaction between aggregating polyGA and ubiquilin 2 may be an early event.

In contrast to ubiquilin 2 co-aggregation with large stellate DPR proteins in the GCL, small neuritic ubiquilin 2 aggregates in *C9orf72*-linked cases punctuated the ML and CA – dendritic layers seemingly independent of a nucleating protein. The neurites in which these small aggregates are found likely derive from the granule or pyramidal cells, respectively,[80,81] therefore DPR protein inclusions in the somata may promote the aggregation of ubiquilin 2 in the dendrites of the same cell. DPR aggregates can sequester proteasome components[82-84] and loss of C9orf72 protein function in cells expressing the DPR-encoding variant 2[85] can impair autophagy,[86-91] which may underpin wild-type ubiquilin 2 aggregation in the ML and CA – dendritic layers in *C9orf72*-linked cases. Further research is required to clarify the relationship between DPR protein and ubiquilin 2 aggregation.

Mutant ubiquilin 2 pathology in *UBQLN2*-linked cases: a neuropathological signature

Even in its wild-type state, ubiquilin 2 intrinsically self-assembles[3] but there is now ample biophysical evidence demonstrating that mutations to ubiquilin 2 confer an increased propensity to oligomerize and undergo aberrant LLPS, forming insoluble aggregates within the cell.[8,9,15,92-94] Here we confirm, albeit in a small number of cases, that mutant ubiquilin 2 in the human hippocampal ML (granule cell dendrites) and CA – l-m/rad layers (pyramidal cell dendrites) is aggregated under less permissive conditions than wild-type ubiquilin 2, appearing to require no aggregated protein scaffold or protein aggregation event in the granule or pyramidal cell soma.

Our study additionally found that p62 labelling was required, while pTDP-43 labelling was dispensable, to confirm cases as being *UBQLN2*-linked. P62 co-localizes with pTDP-43 aggregates and DPR proteins in ALS/FTD[64,95,96] or with hyperphosphorylated tau in a range of tauopathies[97-99] or with mutant α-synuclein in synucleinopathies.[99,100] Given this promiscuity for substrates, discrimination between mutant and wild-type ubiquilin 2 by p62 suggests that there are unique structural or biochemical features of mutant ubiquilin 2 aggregates. However, mutant ubiquilin 2 aggregates may be devoid of p62 co-labelling in the hippocampal ML, albeit rarely (Supplementary Fig. 6A, green arrows) and wild-type ubiquilin 2 aggregates in cellular and rodent overexpression models can be p62-labelled.[101-103] Further research is therefore required to determine whether mutant ubiquilin 2 is structurally distinct enough from wild-type to enable its selective therapeutic targeting.

Beyond the neuropathological signature shared by *UBQLN2*-linked ALS/FTD cases, differences between cases in aggregation patterns and load may reflect differences in the aggregation propensity conferred by specific amino acid substitutions. For example, a much higher ubiquilin 2 aggregate load was observed in cases harbouring a p.P497L variant [Fig. 4D(i)–F(i)] than in those carrying p.T487I, p.P506S or even p.P497H variants. However, heterogeneity was observed even within families carrying the same variant, suggesting further individual level variability. For example, Cases V:7 – T487I and II:3 – P497L had GCL pTDP-43 aggregates while their respective relatives Cases MN17 – T487I, III:3 – P497L and IV:2 – P497L did not. Finally, given that all cases other than Case V:7 – T487I were female, individual variability in aggregation patterns and load may reflect variable skewing of X-inactivation towards wild-type or mutant ubiquilin 2 expression.

In addition to mechanistic insights, the mutant ubiquilin 2 neuropathological signature we describe will enable classification of *UBQLN2* variants of uncertain significance, clarifying the implications of a positive genetic result in a patient. Currently, only six missense variants in *UBQLN2* are designated by ClinVar as pathogenic or likely pathogenic (resulting in p.M392V, p.Q425R, p.P497H, p.P497S, p.P506T and P506L) [https://www.ncbi.nlm.nih.gov/clinvar (accessed 27 November 2023)[104]]. However, 64 other *UBQLN2* missense variants listed in ClinVar are classified as benign or of uncertain significance, including c.1490C>T resulting in p.P497L and c.1516C>T resulting in p.P506S. Indeed, neither *UBQLN2* p.S222G nor p.T487I are even listed in ClinVar, leaving individual diagnostics labs to perform classification for patient reporting. We now confirm that two ALS/FTD cases with a p.T487I variant and three with a p.P497L variant (where both variants segregate with disease in their respective kindreds and show early onset in males, consistent with X-linked disease) shared our newly identified mutant ubiquilin 2 neuropathological signature, supporting their classification as pathogenic variants. Conversely, a male progressive supranuclear palsy (PSP) case with p.S222G who lived to 93 years despite X-linked diseases usually manifesting early in males, did not share this signature, suggesting this variant is benign with respect to ALS/FTD pathogenesis. It is possible that *UBQLN2* variants will prove to be causative of other neurodegenerative diseases, given that ubiquilin 2 co-localizes with aggregates in Parkinson's disease[105] and Huntington's disease[106] and that the clinical spectrum of *UBQLN2*-linked diseases already includes Madras motor neuron disease (p.M392L)[30] and hereditary spastic paraplegia (p.P506S).[11] We encourage uptake of this hippocampal ubiquilin 2 neuropathology signature, by other labs or in collaboration with the authors hereof, as a tool to explore *UBQLN2* variant pathogenicity in ALS/FTD and to understand the applicability of this signature to other diseases.

Conclusion

Ubiquilin 2 aggregates were seen in the hippocampus of ALS/FTD cases across a range of genotypes. Wild-type ubiquilin 2 *in vitro* is known to be aggregation-prone; in human brain it co-aggregated with polyGA, but not pTDP-43 and showed little co-aggregation with p62. Mutant ubiquilin 2 *in vitro* is known to be more aggregation-prone than wild-type; in brain it was either co-aggregated with pTDP-43 or aggregated independently of a known scaffold and appeared to promote the co-aggregation of p62. This hippocampal ubiquilin 2 neuropathology signature provides the foundations of a framework for exploring the biological implications of *UBQLN2* genetic variation and demonstrates that ubiquilin 2 aggregation is likely to play a mechanistic role in *C9orf72*-linked and *UBQLN2*-linked ALS/FTD.

Data availability

The datasets used and/or analysed during the current study are available from the corresponding author on reasonable request.

Acknowledgements

This publication is dedicated to the incredible patients and families who contribute to our research. We thank Marika Eszes at the Centre for Brain Research, University of Auckland, New Zealand; Nailah Siddique at the Northwestern University Feinberg School of Medicine, Chicago, USA; Sashika Selvaduncko and Claire Troakes at the London Neurodegenerative Diseases Brain Bank and Brains for Dementia; and the Neurological Foundation of New Zealand for their ongoing financial support of the Human Brain Bank. We also thank Fairlie Hinton and Dr Catriona McLean at the Victorian Brain Bank, which is supported by The Florey Institute of Neuroscience and Mental Health, The Alfred and the Victorian Forensic Institute of Medicine and funded in part by Parkinson's Victoria, MND Victoria, FightMND and Yulgilbar Foundation. The imaging data reported in this paper were obtained at the Biomedical Imaging Research Unit (BIRU), operated by the Faculty of Medical and Health Sciences' Technical Services at the University of Auckland.

Funding

K.M.T. was funded by a doctoral scholarship from Amelia Pais-Rodriguez and Marcus Gerbich. B.V.D. and M.D. were funded by the Michael J Fox Foundation for Parkinson's Research (Grant ID: 16420). B.V.D. was also funded by a Health Research Council Sir Charles Hercus Health Research Fellowship (21/034). E.L.S. was supported by Marsden FastStart and Rutherford Discovery Fellowship funding from the Royal Society of New Zealand (15-UOA-157, 15-UOA-003). This work was also supported by the Jay C. and Lucile L. Kahn Chair in Alzheimer's Disease Research and Education (to K.L.N.) and grants from Sir Thomas and Lady Duncan Trust and the Coker Family Trust (to M.D.), National Health and Medical Research Council (2011120 to K.L.W.), and from Motor Neuron Disease NZ, Freemasons Foundation, Matteo de Nora, and PaR NZ Golfing (to E.L.S.). No funding body played any role in the design of the study, nor in the collection, analysis or interpretation of data nor in writing the manuscript.

Competing interests

The authors report no competing interests.

Supplementary material

Supplementary material is available at *Brain* online.

References

1. Deng HXX, Chen W, Hong STT, et al. Mutations in UBQLN2 cause dominant X-linked juvenile and adult-onset ALS and ALS/dementia. *Nature*. 2011;477:211-215.
2. Marín I. The ubiquilin gene family: Evolutionary patterns and functional insights. *BMC Evol Biol*. 2014;14:63.
3. Hjerpe R, Bett JS, Keuss MJ, et al. UBQLN2 mediates autophagy-independent protein Aggregate clearance by the proteasome. *Cell*. 2016;166:935-949.
4. Itakura E, Zavodszky E, Shao S, Wohlever ML, Keenan RJ, Hegde RS. Ubiquilins chaperone and triage mitochondrial membrane proteins for degradation. *Mol Cell*. 2016;63:21-33.
5. Protter DSW, Parker R. Principles and properties of stress granules. *Trends Cell Biol*. 2016;26:668-679.
6. Wu JJ, Cai A, Greenslade JE, et al. ALS/FTD mutations in UBQLN2 impede autophagy by reducing autophagosome acidification through loss of function. *Proc Natl Acad Sci U S A*. 2020;117:15230-15241.
7. Alexander EJ, Niaki AG, Zhang T, et al. Ubiquilin 2 modulates ALS/FTD-linked FUS–RNA complex dynamics and stress granule formation. *Proc Natl Acad Sci U S A*. 2018;115:E11485-E11494.
8. Dao TP, Kolaitis RM, Kim HJ, et al. Ubiquitin modulates liquid-liquid phase separation of UBQLN2 via disruption of multivalent interactions. *Mol Cell*. 2018;69:965-978.e6.
9. Sharkey LM, Safren N, Pithadia AS, et al. Mutant UBQLN2 promotes toxicity by modulating intrinsic self-assembly. *Proc Natl Acad Sci U S A*. 2018;115:E10495-E10504.
10. Subudhi I, Shorter J. Ubiquilin 2: Shuttling clients out of phase? *Mol Cell*. 2018;69:919-921.
11. Gkazi SA, Troakes C, Topp S, et al. Striking phenotypic variation in a family with the P506S UBQLN2 mutation including amyotrophic lateral sclerosis, spastic paraplegia, and frontotemporal dementia. *Neurobiol Aging*. 2019;73:229.e5-229.e9.
12. Williams KL, Warraich ST, Yang S, et al. UBQLN2/ubiquilin 2 mutation and pathology in familial amyotrophic lateral sclerosis. *Neurobiol Aging*. 2012;33:2527.e3-2527.e10.
13. McCann EP, Williams KL, Fifita JA, et al. The genotype-phenotype landscape of familial amyotrophic lateral sclerosis in Australia. *Clin Genet*. 2017;92:259-266.
14. Chang L, Monteiro MJ. Defective proteasome delivery of polyubiquitinated proteins by ubiquilin-2 proteins containing ALS mutations. *PLoS One*. 2015;10:1-15.
15. Dao TP, Martyniak B, Canning AJ, et al. ALS-Linked Mutations affect UBQLN2 oligomerization and phase separation in a position- and amino acid-dependent manner. *Structure*. 2019;27:937-951.e5.
16. Gilpin KM, Chang L, Monteiro MJ. ALS-linked mutations in ubiquilin-2 or hnRNPA1 reduce interaction between ubiquilin-2 and hnRNPA1. *Hum Mol Genet*. 2015;24:2565-2577.
17. Higgins N, Lin B, Monteiro MJ. Lou Gehrig's disease (ALS): UBQLN2 mutations strike out of phase. *Structure*. 2019;27:879-881.
18. Chen J, Liu X, Xu Y, Fan D. Association between rare UBQLN2 variants and amyotrophic lateral sclerosis in Chinese population. *Natl Med J China*. 2021;101:846-850.
19. Kim H jung J, Kwon M jung J, Choi W jun J, et al. Mutations in UBQLN2 and SIGMAR1 genes are rare in Korean patients with amyotrophic lateral sclerosis. *Neurobiol Aging*. 2014;35:1957.e7-1957.e8.
20. Baglivo M, Manara E, Capodicasa N, et al. Early-onset of frontotemporal dementia and amyotrophic lateral sclerosis in an Albanian patient with a c.1319C>T variant in the UBQLN2 gene. *Open Med J*. 2020;7:25-31.
21. Daoud H, Suhail H, Szuto A, et al. UBQLN2 mutations are rare in French and French-Canadian amyotrophic lateral sclerosis. *Neurobiol Aging*. 2012;33:2230.e1-2230.e5.
22. Dillen L, van Langenhove T, Engelborghs S, et al. Explorative genetic study of UBQLN2 and PFN1 in an extended Flanders-Belgian cohort of frontotemporal lobar degeneration patients. *Neurobiol Aging*. 2013;34:1711.e1-1711.e5.
23. Gellera C, Tiloca C, del Bo R, et al. Ubiquilin 2 mutations in Italian patients with amyotrophic lateral sclerosis and frontotemporal dementia. *J Neurol Neurosurg Psychiatry*. 2013;84:183-187.
24. Huang X, Shen S, Fan D. No evidence for pathogenic role of UBQLN2 mutations in sporadic amyotrophic lateral sclerosis in the mainland Chinese population. *PLoS One*. 2017;12:1-5.

25. Lattante S, le Ber I, Camuzat A, Pariente J, Brice A, Kabashi E. Screening UBQLN-2 in French frontotemporal lobar degeneration and frontotemporal lobar degeneration-amyotrophic lateral sclerosis patients. *Neurobiol Aging*. 2013;34:2078.e5-2078.e6.
26. Luukkainen L, Helisalmi S, Kytövuori L, et al. Mutation analysis of the genes linked to early onset Alzheimer's disease and frontotemporal lobar degeneration. *J Alzheimers Dis*. 2019;69: 775-782.
27. McLaughlin RL, Kenna KP, Vajda A, et al. UBQLN2 mutations are not a frequent cause of amyotrophic lateral sclerosis in Ireland. *Neurobiol Aging*. 2014;35:267.e9-267.e11.
28. Millecamps S, Corcia P, Cazeneuve C, et al. Mutations in UBQLN2 are rare in French amyotrophic lateral sclerosis. *Neurobiol Aging*. 2012;33:839.e1-839.e3.
29. Morgan S, Shatunov A, Sproviero W, et al. A comprehensive analysis of rare genetic variation in amyotrophic lateral sclerosis in the UK. *Brain*. 2017;140:1611-1618.
30. Özoğuz A, Uyan Ö, Birdal G, et al. The distinct genetic pattern of ALS in Turkey and novel mutations. *Neurobiol Aging*. 2015; 36:1764.e9-1764.e18.
31. Synofzik M, Maetzler W, Grehl T, et al. Screening in ALS and FTD patients reveals 3 novel UBQLN2 mutations outside the PXX domain and a pure FTD phenotype. *Neurobiol Aging*. 2012;33:2949.e13-2949.e17.
32. Teyssou E, Chartier L, Amador MDM, et al. Novel UBQLN2 mutations linked to amyotrophic lateral sclerosis and atypical hereditary spastic paraplegia phenotype through defective HSP70-mediated proteolysis. *Neurobiol Aging*. 2017;58(March): 239.e11-239.e20.
33. Tripolszki K, Gampawar P, Schmidt H, et al. Comprehensive genetic analysis of a Hungarian amyotrophic lateral sclerosis cohort. *Front Genet*. 2019;10:732.
34. Ugwu F, Rollinson S, Harris J, et al. A UBQLN2 variant of unknown significance in frontotemporal lobar degeneration. *Neurobiol Aging*. 2015;36:546.e15-546.e16.
35. Vengoechea J, David MP, Yaghi SR, Carpenter L, Rudnicki SA. Clinical variability and female penetrance in X-linked familial FTD/ALS caused by a P506S mutation in UBQLN2. *Amyotroph Lateral Scler Frontotemporal Degener*. 2013;14(7–8):615-619.
36. Vildan C, Sule D, Turker B, Hilmi U, Sibel KB. Genetic alterations of C9orf72, SOD1, TARDBP, FUS, and UBQLN2 genes in patients with amyotrophic lateral sclerosis. *Cogent Med*. 2019;6:1-10.
37. Fahed AC, McDonough B, Gouvion CM, et al. UBQLN2 mutation causing heterogeneous X-linked dominant neurodegeneration. *Ann Neurol*. 2014;75:793-798.
38. Scotter EL, Smyth L, Bailey JWT, et al. C9ORF72 and UBQLN2 mutations are causes of amyotrophic lateral sclerosis in New Zealand: A genetic and pathologic study using banked human brain tissue. *Neurobiol Aging*. 2017;49:214.e1-214.e5.
39. Nementzik LR, Thumbadoo KM, Murray HC, et al. Distribution of ubiquilin 2 and TDP-43 aggregates throughout the CNS in UBQLN2 p.T487I-linked amyotrophic lateral sclerosis and frontotemporal dementia. *Brain Pathol*. 2024;34(3):e13230.
40. Brettschneider J, van Deerlin VM, Robinson JL, et al. Pattern of ubiquilin pathology in ALS and FTLD indicates presence of C9ORF72 hexanucleotide expansion. *Acta Neuropathol*. 2012; 123:825-839.
41. Arai T, Hasegawa M, Akiyama H, et al. TDP-43 is a component of ubiquitin-positive tau-negative inclusions in frontotemporal lobar degeneration and amyotrophic lateral sclerosis. *Biochem Biophys Res Commun*. 2006;351:602-611.
42. Kwiatkowski TJ, Bosco DA, LeClerc AL, et al. Mutations in the FUS/TLS gene on chromosome 16 cause familial amyotrophic lateral sclerosis. *Science*. 2009;323:1205-1208.
43. Maruyama H, Morino H, Ito H, et al. Mutations of optineurin in amyotrophic lateral sclerosis. *Nature*. 2010;465:223-226.
44. Neumann M, Sampathu DM, Kwong LK, et al. Ubiquitinated TDP-43 in frontotemporal lobar degeneration and amyotrophic lateral sclerosis. *Science*. 2006;314:130-133.
45. Vance C, Rogelj B, Hortobagyi T, et al. Mutations in FUS, an RNA processing protein, cause familial amyotrophic lateral sclerosis type 6. *Science*. 2009;323:1208-1211.
46. Henden L, Wakeham D, Bahlo M. XIBD: Software for inferring pairwise identity by descent on the X chromosome. *Bioinformatics*. 2016;32:2389-2391.
47. Li H, Glusman G, Hu H, et al. Relationship estimation from whole-genome sequence data. *PLoS Genet*. 2014;10:e1004144.
48. Ramstetter MD, Dyer TD, Lehman DM, et al. Benchmarking relatedness inference methods with genome-wide data from thousands of relatives. *Genetics*. 2017;207:75-82.
49. Waldvogel HJ, Bullock JY, Synek BJ, Curtis MA, van Roon-Mom WMC, Faull RLM. The collection and processing of human brain tissue for research. *Cell Tissue Bank*. 2008;9:169-179.
50. Keogh MJ, Wei W, Wilson I, et al. Genetic compendium of 1511 human brains available through the UK medical research council brain banks network resource. *Genome Res*. 2017;27:165-173.
51. Murray HC, Johson K, Sedlock A, et al. Lamina-specific immunohistochemical signatures in the olfactory bulb of healthy, Alzheimer's and Parkinson's disease patients. *Commun Biol*. 2021;5:88.
52. Waldvogel HJ, Curtis MA, Baer K, Rees MI, Faull RLM. Immunohistochemical staining of post-mortem adult human brain sections. *Nat Protoc*. 2007;1:2719-2732.
53. Maric D, Jahanipour J, Li XR, et al. Whole-brain tissue mapping toolkit using large-scale highly multiplexed immunofluorescence imaging and deep neural networks. *Nat Commun*. 2021; 12:1550.
54. Liu F, Morderer D, Wren MC, et al. Proximity proteomics of C9orf72 dipeptide repeat proteins identifies molecular chaperones as modifiers of poly-GA aggregation. *Acta Neuropathol Commun*. 2022;10:1-18.
55. Neumann M, Kwong LK, Lee EB, et al. Phosphorylation of S409/410 of TDP-43 is a consistent feature in all sporadic and familial forms of TDP-43 proteinopathies. *Acta Neuropathol*. 2009;117:137-149.
56. Luisier F, Vonesch C, Blu T, Unser M. Fast interscale wavelet denoising of Poisson-corrupted images. *Signal Processing*. 2010;90:415-427.
57. Brettschneider J, Del Tredici K, Toledo JB, et al. Stages of pTDP-43 pathology in amyotrophic lateral sclerosis. *Ann Neurol*. 2013;74:20-38.
58. Mackenzie IRA, Arzberger T, Kremmer E, et al. Dipeptide repeat protein pathology in C9ORF72 mutation cases: Clinicopathological correlations. *Acta Neuropathol*. 2013;126:859-879.
59. Gorrie GH, Fecto F, Radzicki D, et al. Dendritic spinopathy in transgenic mice expressing ALS/dementia-linked mutant UBQLN2. *Proc Natl Acad Sci U S A*. 2014;111:14524-14529.
60. Ravits J, Appel S, Baloh RH, et al. Deciphering amyotrophic lateral sclerosis: What phenotype, neuropathology and genetics are telling us about pathogenesis. *Amyotroph Lateral Scler Frontotemporal Degener*. 2013;14(sup1):5-18.
61. Nguyen HP, Van Broeckhoven C, van der Zee J. ALS genes in the genomic era and their implications for FTD. *Trends Genet*. 2018; 34:404-423.
62. Taylor JP, Brown RH, Cleveland DW. Decoding ALS: From genes to mechanism. *Nature*. 2016;539:197-206.
63. Ling SC, Polymenidou M, Cleveland DW. Converging mechanisms in ALS and FTD: Disrupted RNA and protein homeostasis. *Neuron*. 2013;79:416-438.

64. Mori K, Weng SM, Arzberger T, et al. The C9orf72 GGGGCC repeat is translated into aggregating dipeptide-repeat proteins in FTLD/ALS. *Science*. 2013;339:1335-1338.
65. Mori K, Arzberger T, Grässer FA, et al. Bidirectional transcripts of the expanded C9orf72 hexanucleotide repeat are translated into aggregating dipeptide repeat proteins. *Acta Neuropathol*. 2013;126:881-893.
66. Shibata N, Hirano A, Kobayashi M, et al. Intense superoxide dismutase-1 immunoreactivity in intracytoplasmic hyaline inclusions of familial amyotrophic lateral sclerosis with posterior column involvement. *J Neuropathol Exp Neurol*. 1996;55:481-490.
67. Bruijn LI, Houseweart MK, Kato S, et al. Aggregation and motor neuron toxicity of an ALS-linked SOD1 mutant independent from wild-type SOD1. *Science*. 1998;281:1851-1854.
68. Keith JL, Swinkin E, Gao A, et al. Neuropathologic description of CHCHD10 mutated amyotrophic lateral sclerosis. *Neurol Genet*. 2020;6:e394.
69. Smith BN, Topp SD, Fallini C, et al. Mutations in the vesicular trafficking protein annexin A11 are associated with amyotrophic lateral sclerosis. *Sci Transl Med*. 2017;9:eaad9157.
70. Smith BN, Vance C, Scotter EL, et al. Novel mutations support a role for profilin 1 in the pathogenesis of ALS. *Neurobiol Aging*. 2015;36:1602.e17-1602.e27.
71. Teyssou E, Takeda T, Lebon V, et al. Mutations in SQSTM1 encoding p62 in amyotrophic lateral sclerosis: Genetics and neuropathology. *Acta Neuropathol*. 2013;125:511-522.
72. Hirsch-Reinshagen V, Pottier C, Nicholson AM, et al. Clinical and neuropathological features of ALS/FTD with TIA1 mutations. *Acta Neuropathol Commun*. 2017;5:96.
73. Tada M, Doi H, Koyano S, et al. Matrin 3 is a component of neuronal cytoplasmic inclusions of motor neurons in sporadic amyotrophic lateral sclerosis. *Am J Pathol*. 2018;188:507-514.
74. van Deerlin VM, Leverenz JB, Bekris LM, et al. TARDBP mutations in amyotrophic lateral sclerosis with TDP-43 neuropathology: A genetic and histopathological analysis. *Lancet Neurol*. 2008;7:409-416.
75. Tan RH, Kril JJ, Fatima M, et al. TDP-43 proteinopathies: Pathological identification of brain regions differentiating clinical phenotypes. *Brain*. 2015;138:3110-3122.
76. McEachin ZT, Gendron TF, Raj N, et al. Chimeric peptide Species contribute to divergent dipeptide repeat pathology in c9ALS/FTD and SCA36. *Neuron*. 2020;107:292-305.e6.
77. Freibaum BD, Taylor JP. The role of dipeptide repeats in C9ORF72-related ALS-FTD. *Front Mol Neurosci*. 2017;10(February):1-9.
78. Lee YB, Baskaran P, Gomez-Deza J, et al. C9orf72 poly GA RAN-translated protein plays a key role in amyotrophic lateral sclerosis via aggregation and toxicity. *Hum Mol Genet*. 2017;26:4765-4777.
79. Nonaka T, Masuda-Suzukake M, Hosokawa M, et al. C9ORF72 dipeptide repeat poly-GA inclusions promote intracellular aggregation of phosphorylated TDP-43. *Hum Mol Genet*. 2018;27:2658-2670.
80. Lindsay RD, Scheibel AB. Quantitative analysis of dendritic branching pattern of granular cells from human dentate gyrus. *Exp Neurol*. 1976;52:295-310.
81. Amaral DG, Scharfman HE, Lavenex P. The dentate gyrus: Fundamental neuroanatomical organization (dentate gyrus for dummies). *Prog Brain Res*. 2007;163:3-790.
82. May S, Hornburg D, Schludi MH, et al. C9orf72 FTLD/ALS-associated Gly-Ala dipeptide repeat proteins cause neuronal toxicity and Unc119 sequestration. *Acta Neuropathol*. 2014;128:485-503.
83. Gupta R, Lan M, Mojsilovic-Petrovic J, et al. The proline/arginine dipeptide from hexanucleotide repeat expanded C9ORF72 inhibits the proteasome. *eNeuro*. 2017;4:ENEURO.0249-16.2017.
84. Zhang YJ, Gendron TF, Grima JC, et al. C9ORF72 poly(GA) aggregates sequester and impair HR23 and nucleocytoplasmic transport proteins. *Nat Neurosci*. 2016;19:668-677.
85. van Blitterswijk M, Gendron TF, Baker MC, et al. Novel clinical associations with specific C9ORF72 transcripts in patients with repeat expansions in C9ORF72. *Acta Neuropathol*. 2015;130:863-876.
86. Webster CP, Smith EF, Bauer CS, et al. The C9orf72 protein interacts with Rab1a and the ULK 1 complex to regulate initiation of autophagy. *EMBO J*. 2016;35:1656-1676.
87. Wang M, Wang H, Tao Z, et al. C9orf72 associates with inactive rag GTPases and regulates mTORC1-mediated autophagosomal and lysosomal biogenesis. *Aging Cell*. 2020;19:1-14.
88. Boivin M, Pfister V, Gaucherot A, et al. Reduced autophagy upon C9ORF72 loss synergizes with dipeptide repeat protein toxicity in G4C2 repeat expansion disorders. *EMBO J*. 2020;39:1-15.
89. Zhu Q, Jiang J, Gendron TF, et al. Reduced C9ORF72 function exacerbates gain of toxicity from ALS/FTD-causing repeat expansion in C9orf72. *Nat Neurosci*. 2020;23(May):615-624.
90. Beckers J, Tharkeshwar AK, van Damme P. C9orf72 ALS-FTD: Recent evidence for dysregulation of the autophagy-lysosome pathway at multiple levels. *Autophagy*. 2021;00:1-17.
91. Sellier C, Campanari M, Julie Corbier C, et al. Loss of C9ORF72 impairs autophagy and synergizes with polyQ ataxin-2 to induce motor neuron dysfunction and cell death. *EMBO J*. 2016;35:1276-1297.
92. Renaud L, Picher-Martel V, Codron P, Julien JP. Key role of UBQLN2 in pathogenesis of amyotrophic lateral sclerosis and frontotemporal dementia. *Acta Neuropathol Commun*. 2019;7:103.
93. Zhang KY, Yang S, Warraich ST, Blair IP. Ubiquilin 2: A component of the ubiquitin-proteasome system with an emerging role in neurodegeneration. *Int J Biochem Cell Biol*. 2014;50:123-126.
94. Sharkey LM, Sandoval-Pistorius SS, Moore SJ, et al. Modeling UBQLN2-mediated neurodegenerative disease in mice: Shared and divergent properties of wild type and mutant UBQLN2 in phase separation, subcellular localization, altered proteostasis pathways, and selective cytotoxicity. *Neurobiol Dis*. 2020;143(June):105016.
95. Mann DM, Rollinson S, Robinson A, et al. Dipeptide repeat proteins are present in the p62 positive inclusions in patients with frontotemporal lobar degeneration and motor neurone disease associated with expansions in C9ORF72. *Acta Neuropathol Commun*. 2013;1:68.
96. Al-Sarraj S, King A, Troakes C, et al. P62 positive, TDP-43 negative, neuronal cytoplasmic and intranuclear inclusions in the cerebellum and hippocampus define the pathology of C9orf72-linked FTLD and MND/ALS. *Acta Neuropathol*. 2011;122:691-702.
97. Piras A, Collin L, Grüninger F, Graff C, Rönnbäck A. Autophagic and lysosomal defects in human tauopathies: Analysis of postmortem brain from patients with familial Alzheimer disease, corticobasal degeneration and progressive supranuclear palsy. *Acta Neuropathol Commun*. 2016;4:22.
98. Babu JR, Geetha T, Wooten MW. Sequestosome 1/p62 shuttles polyubiquitinated tau for proteasomal degradation. *J Neurochem*. 2005;94:192-203.
99. Zatloukal K, Stumptner C, Fuchsbichler A, et al. P62 is a common component of cytoplasmic inclusions in protein aggregation diseases. *Am J Pathol*. 2002;160:255-263.

100. Kuusisto E, Salminen A, Alafuzoff I. Ubiquitin-binding protein p62 is present in neuronal and glial inclusions in human tauopathies and synucleinopathies. *Neuroreport*. 2001;12:2085-2090.
101. Ceballos-Diaz C, Rosario AM, Park HJ, et al. Viral expression of ALS-linked ubiquilin-2 mutants causes inclusion pathology and behavioral deficits in mice. *Mol Neurodegener*. 2015;10:1-13.
102. Mohan HM, Trzeciakiewicz H, Pithadia A, et al. RTL8 promotes nuclear localization of UBQLN2 to subnuclear compartments associated with protein quality control. *Cell Mol Life Sci*. 2022;79:176.
103. Osaka M, Ito D, Yagi T, Nihei Y, Suzuki N. Evidence of a link between ubiquilin 2 and optineurin in amyotrophic lateral sclerosis. *Hum Mol Genet*. 2015;24:1617-1629.
104. Richards S, Aziz N, Bale S, et al. Standards and guidelines for the interpretation of sequence variants: A joint consensus recommendation of the American college of medical genetics and genomics and the association for molecular pathology. *Genet Med*. 2015;17:405-424.
105. Mori F, Tanji K, Odagiri S, et al. Ubiquilin immunoreactivity in cytoplasmic and nuclear inclusions in synucleinopathies, polyglutamine diseases and intranuclear inclusion body disease. *Acta Neuropathol*. 2012;124:149-151.
106. Rutherford NJ, Lewis J, Clippinger AK, et al. Unbiased screen reveals ubiquilin-1 and -2 highly associated with huntingtin inclusions. *Brain Res*. 2013;1524:62-73.